Low-frequency Vibrational Anomalies in β-Lactoglobulin: Contribution of Different Hydrogen Classes Revealed by Inelastic Neutron Scattering

A. Orecchini, A. Paciaroni, A. R. Bizzarri, and S. Cannistraro*

INFM, Dipartimento di Scienze Ambientali, Università della Tuscia, I-01100 Viterbo, Italy

Received: April 19, 2001; In Final Form: September 21, 2001

The low-frequency dynamics of the globular protein β-lactoglobulin has been investigated by inelastic neutron scattering, on both dry and D_2O-hydrated samples. Both the dynamic structure factor and the density of states display an excess of vibrational modes with respect to the Debye level, with such an excess being reminiscent of the so-called boson peak. To establish which protein structural elements give origin to the anomalous peak, the samples were submitted to suitable H/D exchange procedures, which allowed us to highlight the following points: (i) in the dry samples, nonexchangeable, internal, hydrogens display a peak at 3 meV; (ii) exchangeable, mainly external, hydrogens provide a further peak, which is shifted to lower frequencies and displays a stronger intensity per atom; (iii) in the hydrated samples, no frequency difference between the peaks of external and internal hydrogens is found, meanwhile the stronger scattering intensity due to external hydrogens is still observed. These results are discussed in the framework of a model ascribing the anomalous bump to interactions of acoustic phonons with density fluctuations domains and the effect of hydration on the protein dynamics is revisited.

Introduction

Conformational changes of proteins, an essential requirement to their function, are known to be driven by molecular motions and influenced by the dynamics of hydration water. Therefore, the study and understanding of protein dynamical behavior is of extreme interest. In biological molecules, particularly important dynamical contributions arise from picosecond motions, with corresponding energies of about 0.1−10 meV, and this dynamical regime is often referred to as *low-frequency* range.[1,2] Because of its typically accessible energy and momentum transfers, inelastic thermal neutron scattering is probably the most powerful experimental technique for studying such low-frequency modes.

Within this dynamical range, a puzzling feature is still attracting great interest. The low-temperature dynamic structure factor of proteins, as obtained by inelastic neutron scattering and Raman spectroscopy, shows the presence of a large vibrational peak centered at about 2−4 meV.[1,3−10] Upon increasing the temperature, such a peak becomes less distinguishable because of the rise of a quasielastic broad band,[3−8] which is suggested to be connected to an overdamping of the inelastic bump.[11−12] Such a bump is also known to be affected by the hydration degree of the molecule: with increasing hydration level, the peak shifts to higher frequencies and its intensity is depressed.[3,5,8] Moreover, a recent neutron scattering experiment[13] has proven the existence of the same bump in the protein hydration water also, suggesting a dynamical coupling between biomolecules and their hydration shell.

Actually, the same spectral feature, with a similar temperature dependence, was first observed as a general characteristic of glassy materials, where it is often referred to as *boson peak.*[14−19] Indeed, the strong analogy between proteins and glasses is well-known and relies on the fact that these two classes of systems share many physical properties.[20−22] Besides the boson peak, we can remember the anomalous specific heat, the peculiar behavior of some relaxation processes, and the occurrence of a dynamical (glass) transition witnessed by the temperature dependence of the atom mean-square displacements; in proteins, such transition having been suggested to be slaved to the solvent.[1,8,22] The origin of such analogy has been ascribed to the fact that both systems are characterized by a complex energy hypersurface, with a huge number of nearly isoenergetic valleys, and can thus assume many conformational substates.[20] In biomolecules, a rise of temperature in hydrated samples allows the system to explore an increasing number of such substates, thus triggering the onset of large amplitude motions, related to the occurrence of the so-called dynamical transition.

Concerning the boson peak, the interest aroused by this vibrational bump is due to the fact that it represents an anomalous, still unexplained, excess of modes with respect to the Debye-like behavior of harmonic systems. In terms of vibrational density of states $g(\omega)$, which can be derived from incoherent inelastic neutron scattering spectra, the boson peak appears as an overshoot in the $g(\omega)/\omega^2$ function. Several attempts have been made at explaining the origin of such anomalous bump. Indeed, its connection with a disordered nature and/or complexity of the system is quite well accepted. Among the proposed models, lattices of atoms connected by a random elastic network have been suggested[23−26] or the involvement of "soft" anharmonic potentials has been invoked.[11,12] Other authors proposed interactions between sound waves and density fluctuations domains to be responsible for a phonon localization at the boson peak frequency.[27−29]

Models developed for amorphous systems have been extended to biomolecules. Furthermore, attempts to attribute the peak vibrations to specific protein structural elements (such as side chains, backbone, α-helices, and β-sheets) are being made. The experimental peak dependence on the protein hydration level led some authors to address librations of solvent-exposed side

* To whom correspondence should be addressed. E-mail: cannistr@unitus.it.

10.1021/jp0114889 CCC: $20.00
Published on Web 11/10/2001

TABLE 1: Protein Hydrogen Classes in βLG

proton class	chemical bond	number of protons
nonexchangeable	CH_n	1068
fast-exchangeable	OH, SH, NH_{amine}	94
slow-exchangeable	NH_{amide}	146

chains as the main responsible for the scattering excess.[5] On the other hand, a recent molecular dynamics (MD) simulation screening suggested that significant contributions should arise from the protein backbone.[30] Moreover, some new experimental results indicated that exchangeable and nonexchangeable hydrogen atoms, located on different regions of the protein and differently exposed to the solvent, can give different contributions to the low-frequency spectral anomaly.[31] Taken together, such findings suggest that a deeper experimental assessment of the role played by the various protein structural elements would be extremely valuable for understanding the origin of the anomalous peak.

In this paper, we report the results of an inelastic neutron scattering experiment we carried out on both dry and D_2O-hydrated samples of β-lactoglobulin. To discriminate between the dynamics of exchangeable hydrogen atoms, essentially located on solvent-exposed residues, and nonexchangeable hydrogen atoms, mainly situated in the protein interior, we submitted our samples to appropriate H/D exchange procedures. Our experimental results provide novel information about the contributions to the anomalous bump arising from external and internal protein residues. These findings are discussed in the framework of the phonon localization model,[27] and the effect of hydration on the protein dynamics is revisited.

Materials and Methods

β-lactoglobulin[32−35] (βLG) is a β-barrel globular protein, which can be extracted from milk whey and is composed by a sequence of 162 amino acids, corresponding to a molecular weight of 18155 Da. Its chemical composition is $C_{820}H_{1308}N_{206}O_{252}S_9$. Our βLG powders were obtained by Sigma Aldrich. The 1308 protein protons can be classified in nonexchangeable, fast-exchangeable, and slow-exchangeable, according to their chemical bond to the protein sequence[36,37] (see Table 1). Exchangeable hydrogens turn out to be 20% of the total amount and are mainly located (∼90%) on the outer shells of the protein structure. To single out contributions to the boson peak arising from the different classes of protein hydrogen atoms, we prepared four samples by the following different procedures. The first sample was prepared by simply dehydrating 301 mg of protein as commercially obtained. The sample was first lyophilized and then desiccated under vacuum in the presence of P_2O_5 for 2 days, achieving a final hydration level lower than $h = 0.05$ g of water per gram of protein. Such sample contains both exchangeable and nonexchangeable protons and, in the following, will be referred to as the **dry** one. In the second sample, all exchangeable protons are wanted to be substituted with deuterium atoms. Therefore, 368 mg of βLG powder was first dissolved in 15 mL of D_2O for 1 week and then lyophilized. These two steps were repeated three times, to achieve a complete proton exchange. Finally, the exchanged protein was desiccated under vacuum with P_2O_5 for 2 days, achieving a final hydration level lower than $h = 0.05$ g of water per gram of protein. We will refer to this second sample as the **dry deuterated** one. The last two samples were obtained by hydrating with D_2O two further dry and dry deuterated powders, prepared by the previously described procedure. The hydration process was carried out in a chamber under vacuum in the presence of a saturated KCl and heavy water solution, achieving a final hydration level of $h = 0.4$ g of D_2O per gram of protein. These two samples will be called in the sequel **D_2O-hydrated** and **D_2O-hydrated deuterated**, respectively. The hydration state of the four samples was carefully checked, both before and after the neutron scattering experiment, and was found to be unchanged.

In a βLG molecule, hydrogen atoms are about 50% of the total amount. Because the hydrogen cross-section is about 1 order of magnitude larger than the cross-sections of deuterium and of the other protein atoms, in a neutron scattering experiment, almost only hydrogens will be visible. Therefore, the comparison between deuterated and nondeuterated samples will discriminate between scattering contributions arising from exchangeable and nonexchangeable protons. Moreover, as the coherent part of the hydrogen cross-section is exceedingly small with respect to the total (∼2%), the scattering will be mainly incoherent. Actually, for a more accurate evaluation of the coherent contribution, all protein atoms should be taken into account. From the stoichiometry of our samples and from tabulated values of the neutron scattering lengths,[38] we can theoretically estimate that the coherent contribution will be not larger than 10−15% of the total cross-section.

In an inelastic neutron scattering experiment on an isotropic sample, the measured quantity is the dynamic structure factor $S(q,\omega)$, where q is the modulus of the momentum transfer and ω is the energy transfer, both in units of $\hbar$. In the one-phonon approximation, the incoherent dynamic structure factor at a given temperature T can be written as the sum of three terms:

$$S(q,\omega) = e^{-2W(q,T)}\{EISF(q)\delta(\omega) + [1 - EISF(q)]S_{QE}(q,\omega)\} + S_{INEL}(q,\omega) \quad (1)$$

where $e^{-2W(q,T)}$ is the Debye−Waller factor, $EISF(q)$ is the elastic incoherent scattering function, $\delta(\omega)$ is the Dirac delta function, $S_{QE}(q,\omega)$ is the quasielastic incoherent dynamic structure factor, and $S_{INEL}(q,\omega)$ is the inelastic incoherent dynamic structure factor.[39] The first term takes into account for the elastic response of the system. In the Gaussian approximation, which holds for low q-values, $EISF(q)$ can be considered as q independent. The second term gives information about diffusive, nonvibrational motions and appears as a broadening of the elastic peak. The last term describes the vibrational behavior of the studied system and, assuming that only incoherent scattering is visible, can be explicitly written

$$S_{INEL}(q,\omega) = e^{-2W(q,T)}\frac{q^2}{8\pi M}\frac{n(\omega,T)}{\omega}g(\omega) \quad (2)$$

where M is the mass of the scattering unit, $n(\omega, T)$ is the Bose factor and $g(\omega)$ is the density of vibrational states. In a real experiment, eq 1 is understood to be convoluted with the energy resolution function of the instrument. If $S_{INEL}(q,\omega)$ is measured, $g(\omega)$ can be obtained by means of eq 2, provided that the factor $W(q, T)$ can be estimated. With this respect, under quite general conditions, the following expression holds:

$$2W(q,T) = \frac{1}{3}\langle u^2(T)\rangle q^2 \quad (3)$$

which can be used to derive the Debye−Waller factor. Here, the quantity $\langle u^2(T)\rangle$ is to be thought of as an average atomic mean-square displacement.

The neutron scattering experiment was performed with the high-flux time-of-flight spectrometer IN6 at Institut Laue-Langevin (ILL) in Grenoble. An incident wavelength of 5.1 Å was chosen, achieving an elastic energy resolution of 70 μeV, a q range from 0.2 to 2.0 Å^{-1} and an accessible energy transfer ranging from -1.9 meV to $2k_BT$. The four samples were placed in standard slab-shaped aluminum cells, whose dimensions were $30 \times 50 \times 0.5$ mm^3. The cells were placed into the neutron flux with an angle of 135° with respect to the incident beam. Spectra were collected at three temperatures for each sample, $T = 100$, 220, and 300 K, for a period of time of about 2−6 h, depending on the temperature. Each spectrum was measured at 89 different scattering angles, in the range $10.3° \leq 2\theta \leq 113.5°$. Moreover, spectra from the empty can and from a cadmium absorber were collected at 300 K, to take into account for the various scattering contributions due to sample environment. A vanadium standard scan was performed in order to measure the resolution function and to take into account for the different detector efficiencies. After having checked and removed those detectors which showed a too high electronic noise, the data reduction was performed using standard ILL programs, which correct spectra for incident flux, cell and environment scattering, electronic noise, detector efficiency, and self-absorption. Moreover, for each spectrum, detectors were binned into five groups of scattering angles, to attain a better statistics. Because all samples have transmissions of about 92%, multiple scattering and multiphonon corrections were not applied. The obtained cross-sections, depending on the scattering angle 2θ and on the energy transfer ω, were then calculated as functions of q and ω, with a standard interpolation procedure which takes into account for the kinematic constraints involving q, 2θ, and ω.

To study possible differences due to the sole dynamical behavior and not to the different number of scatterers between the measured samples, the dynamic structure factors must be normalized to the same scattering unit. When the effect under investigation is as small as in the present case (∼20%), a reliable normalization is very difficult to obtain by simply rescaling each measured cross-section to the mass of the sample. Indeed, systematic errors can be easily introduced if the sample density is not homogeneous all over the cell or if the sample is not uniformly bathed by the neutron flux. Thus, as alternative procedure, the normalized dynamic structure factors were obtained by dividing each corrected cross-section by the low-q limit of its elastic peak (*internal normalization*). In particular, let $S(q) = e^{-2W(q,\,T)}EISF(q)$ denote the elastic part of the dynamic structure factor in eq 1. Using eq 3, the logarithm of $S(q)$ can be written

$$\ln S(q) = \ln EISF(q) - \frac{1}{3}\langle u^2(T)\rangle q^2 \qquad (4)$$

At low q values, where the Gaussian approximation holds (i.e., $EISF(q)$ is q-independent), a linear fit of $\ln S(q)$ vs q^2 provides the quantity $EISF(q = 0)$, the low-q limit needed for normalizing the measured spectra. For q values lower than 0.7 Å^{-1}, our data were found to conform to eq 4 (with $EISF(q) = \text{const}$) to a very good extent. Furthermore, even over the whole q range, oscillations in $EISF(q)$ due to coherent scattering were found to be smaller than 5%, a value actually lower than the theoretical estimate reported above. From the fitting procedure, the average mean-square displacement $\langle u^2(T)\rangle$ is also obtained and can be used to estimate the Debye−Waller factor.

Under the assumption that only vibrational motions are active at low temperature, the density of states $g(\omega)$ has been derived from the normalized spectra at 100 K. The computation of $g(\omega)$ has been performed through the equation

$$g(\omega) = \frac{8\pi M\omega}{n(\omega, T)}\lim_{q\to 0}\left[\frac{S_{\mathrm{INEL}}(q, \omega)}{q^2 e^{-2W(q,\,T)}}\right]$$

where the Debye−Waller factor has been estimated by the previously described fitting procedure.

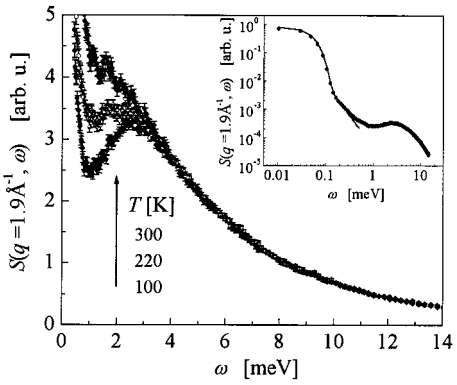

Figure 1. Dynamic structure factor of the dry sample, as function of energy and at $q = 1.9$ Å^{-1}, measured at $T = 100$, 220, and 300 K from bottom to top. The 220 and 300 K spectra have been rescaled by the Bose factor at the common temperature of 100 K. *Inset.* Dynamic structure factor of the dry sample, at $q = 1.9$ Å^{-1} and $T = 100$ K. The bilogarithmic scale emphasizes the elastic peak, which is compared with the resolution function (full line), obtained by the measurement on the vanadium standard.

Results and Discussion

Figure 1 shows the dynamic structure factor of the dry sample, as a function of energy and at fixed momentum transfer $q = 1.9$ Å^{-1}, measured at 100, 220, and 300 K. The 220 and 300 K spectra have been rescaled by the Bose factor at the common temperature of 100 K. As described in the Materials and Methods section, each spectrum can be considered as the sum of three contributions, an elastic, a quasielastic, and an inelastic component. The elastic component is not a delta function, as expected from eq 1, but has a well-defined width because of the finite instrumental energy resolution. Such an effect is emphasized by the bilogarithmic scale of the inset, where the elastic peak of the100 K spectrum is compared with the resolution function (full line), obtained by the measurement of the vanadium standard. Upon increasing the temperature, the elastic intensity decreases (not shown), due to the rise of $\langle u^2(T)\rangle$ in the Debye−Waller factor (see eq 3). Such a decrease is compensated for by both an increasing quasielastic scattering, which appears as a further broadening of the elastic peak and an increasing inelastic scattering. Concerning the inelastic region of the spectrum, at 100 K, it is characterized by a well-defined maximum centered at about 2.7 meV. At 220 K, the maximum is less pronounced, due to its overlapping with the quasielastic scattering, and at 300 K, it is almost completely submerged. In the Debye approximation and at such low frequencies, the vibrational density of states is expected to be proportional to ω^2, which should be canceled out by the two factors $n(\omega, T) \sim k_BT/\omega$ and $1/\omega$ (see eq 2), resulting in a constant $S_{\mathrm{INEL}}(q,\omega)$ as a function of the energy. Therefore, the bump appearing at 100 K represents an anomalous excess of scattering with respect to the Debye level. To better characterize such bump, its q dependence is plotted in Figure 2. As predicted by eq 2, once normalized by the Debye−Waller factor, the bump intensity increases with the square momentum transfer (see inset) thus

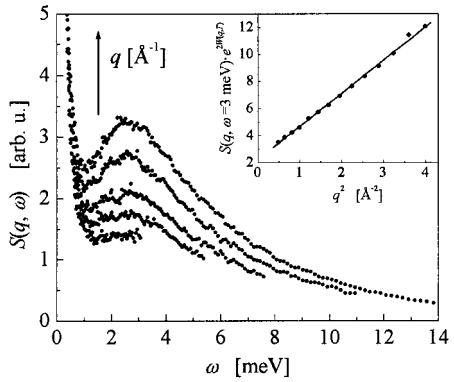

Figure 2. Dynamic structure factor of the dry sample at 100 K, for different values of the momentum transfer: $q = 0.77$, 1.02, 1.24, 1.57, and 1.90 Å^{-1} from bottom to top. Because of kinematic constraints, at lower q values only lower energy transfers can be reached. *Inset.* At the anomalous peak energy (3 meV), the low-temperature (100 K) dynamic structure factor of the dry sample, divided by the Debye−Waller factor, is plotted as function of q^2. The full line is a linear fit of the experimental data.

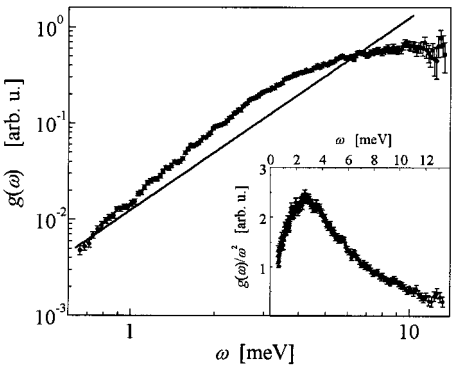

Figure 3. Low-frequency vibrational density of states for the dry sample. The full line, having slope 2 on a bilogarithmic scale, represents the Debye level. *Inset.* Low-frequency vibrational density of states normalized by the Debye-like behavior ω^2.

indicating both its vibrational and incoherent nature. With regard to this latter point in particular, in the previous section, we have estimated a coherent contribution of about 10−15%. This value is referred to the total cross-section, namely, the cross-section integrated over all possible q and ω values. When referring to a limited (q,ω) region, the coherent contribution can actually be much lower. Indeed, the q^2 behavior displayed by the peak witnesses that, at such energies and within the explored q range, negligible coherent scattering is actually present.

The same anomalous bump, with similar temperature behavior and q dependence, has also been observed in other proteins.[1,3−8] Indeed, it is reminiscent of the so-called boson peak, which is a well-known feature of glassy systems. In these materials, this extraintensity is often pointed out as a broad maximum in the $g(\omega)/\omega^2$ function.[11,14,15,18,40] Fewer times, possibly due to low statistics, the density of states $g(\omega)$ has been experimentally determined for biological systems.[4,41] The good quality of the collected data allowed us to obtain the vibrational density of states, according to the Materials and Methods section. The possibility of deriving $g(\omega)$ from the measured $S(q,\omega)$ relies on the assumption that at low temperature, besides the elastic peak, scattering processes are mainly due to vibrational motions, whereas diffusion gives only little contributions. At higher temperatures, the rising quasielastic scattering indicates that diffusion is no more negligible; therefore, $g(\omega)$ can be computed for the 100 K spectrum only. The density of vibrational states of the dry sample is shown in Figure 3 on a bilogarithmic plot. In such a scale, the Debye level ($\propto\omega^2$) is proportional to a line with slope 2 (full line); therefore, the higher slope of the experimental $g(\omega)$ at low frequency indicates that the scattering bump is due to an excess of vibrational states with respect to the Debye level. Such an excess is even better emphasized in the $g(\omega)/\omega^2$ function, which is plotted in the inset and displays a neat maximum at about 2.7 meV.

Concerning the origin of the boson peak in glasses, interactions of acoustic modes with density fluctuations have been suggested as a possible explanation.[27−29] In particular, in the disordered glass structure, the existence of limited density fluctuations domains, within which short- and medium-range order is maintained, has been hypothesized.[27] In this picture, the vibrational anomaly has been ascribed to phonon scattering by such "clusters": phonons localization at the boson peak frequencies would occur when their mean-free path becomes comparable to the size of the domains. In particular, the *minimum* mean-free path would be determined by the domains diameter D, also referred to as the characteristic correlation length of the system, which can be estimated through the equation

$$\nu_0 = \frac{\upsilon_s}{D} \tag{5}$$

where ν_0 is the boson peak frequency and υ_s is the sound velocity.

If such model is extended to proteins,[3,30,42] the characteristic length scale of the vibrations involved in the observed scattering excess can be estimated, provided the sound velocity in biological systems is known. Even if an accurate measurement is not easily attainable, reasonable values for υ_s of about 3000 m/s have been suggested,[43] and accordingly, a *minimum* mean-free path D of about 40 Å can be derived. Such a length scale is comparable with the βLG dimensions (∼40 Å). Recalling that the estimated phonon mean-free path is the *minimum* allowed, such finding suggests that the involved vibrations might propagate through more than one molecule, rather than being confined within a single one. Indeed, both our dry and hydrated samples consist in powders, where the macromolecules are in close contact between them. Such hypothesis should be considered also in connection with the results of a recent MD simulation study,[44] whose authors claim that, among other requirements, interactions between more molecules must be included to correctly reproduce the proteins anomalous bump.

The interpretation of the vibrational excess of modes in terms of localized phonon propagation can also qualitatively account for the hydration dependence of the peak maximum. The effect of hydration on the protein scattering excess is shown in Figure 4, where the measured dynamic structure factors of the dry and D_2O-hydrated samples at 100 K are plotted together. The peak of the hydrated protein is shifted toward higher frequencies and displays a depressed intensity, with this result being in agreement with what has been observed in other biological molecules.[3,5,8] For a small globular protein, it has been shown that hydrated samples are characterized by higher sound velocities than dry ones.[43] In the framework of the previously discussed model, a higher υ_s leads to higher vibrational frequencies, which is consistent with the observed behavior. Actually, the ratio between the observed peak frequencies of the dry (∼2.7 meV) and hydrated (∼3.3 meV) samples is larger than expected from the values of the sound velocities in dry (∼2260 m/s) and wet (∼3300 m/s) proteins.[43] However, such a discrepancy could be due to either the uncertainty in the determination of υ_s or a

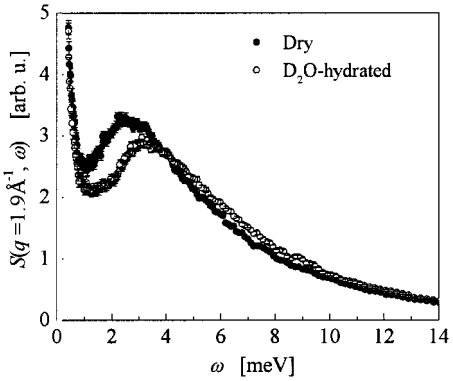

Figure 4. Dynamic structure factors as functions of energy, at $q = 1.9$ Å^{-1} and $T = 100$ K, of the dry (full circles) and D_2O-hydrated (open circles) samples.

concomitant increase of the protein effective diameter in hydrated samples.

Alternative interpretations of the peak hydration dependence address the anomalous bump to vibrations of specific protein structural elements. Early MD simulations suggested that protein−water interactions depress low-frequency modes.[45] On such a basis, the observed hydration dependence has been related to the number and strength of protein−water hydrogen bonds: with increasing water content, the increasing number of hydrogen bonds is expected to strengthen the force constants of the system, leading to higher vibrational frequencies and lower mobility. According to this hypothesis, and to the observation of the anomalous bump in denatured myoglobin and in mixtures of hydrated amino acids, an interpretation in terms of water-coupled librations of solvent-exposed polar side-chains was suggested.[5] On the other hand, a MD simulation study of myoglobin indicated that the scattering excess is mainly due to lateral chains located in the protein inner region.[46] Meanwhile, a recent novel analysis of MD simulation data suggested that the main contribution arises from the protein backbone.[30]

In light of these conflicting results, a clearer assessment of which protein structural elements give origin to the anomalous peak vibrations is highly desirable. With this respect, the H/D exchange procedure can be helpful. Indeed, a NMR study of the βLG structure indicates that regions highly protected from the exchange are those located in the internal core of the protein. On the contrary, the majority (~90%) of exchangeable hydrogens is located on solvent-exposed side-chains.[34] Thus, the isotopic hydrogen exchange could help in discriminating the dynamical behavior of surface and internal residues.

The low-temperature spectra of the dry and dry deuterated samples, together with those of the D_2O-hydrated and D_2O-hydrated deuterated samples, are compared in Figure 5. In this figure, the spectra of the two dry samples are to be referred to the right axis, which is upward-shifted for clearness. The dry deuterated sample, which contains only nonexchangeable hydrogens, exchangeable ones being replaced by deuterium atoms, displays a well defined scattering excess at 3 meV. The dry sample, which, in addition to the previous ones, contains also exchangeable hydrogens, shows a bump which is shifted toward lower frequencies and displays a higher intensity per atom. Such an intensity difference is significant because, as described in the Materials and Methods section, the two spectra were independently normalized to the same scattering unit. From a comparison with the previous spectrum, it can be inferred that exchangeable hydrogens are responsible for an additional excess characterized by lower frequencies (see below for a detailed

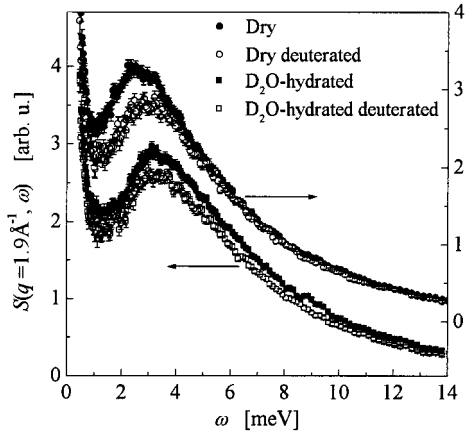

Figure 5. Dynamic structure factors as functions of energy, at $q = 1.9$ Å^{-1} and $T = 100$ K, of the dry (full circles) and dry deuterated (open circles) samples and of the D_2O-hydrated (full squares) and D_2O-hydrated deuterated (open squares) samples. The spectra of the two dry samples are to be referred to the right axis, which is upward-shifted for clarity.

analysis) and higher scattering intensity. A similar exchange-based experiment was performed with dry myoglobin,[5] but in that case, no significant difference was actually observed and an identical dynamical behavior of external and internal atomic groups was deduced. The discrepancy with the results presented herewith can be attributed to a possibly higher statistics achieved with the present experiment, or to a different exchange procedure, or to a peculiar behavior of βLG with respect to myoglobin. On the other hand, a more recent experiment on plastocyanin revealed exchangeable hydrogen atoms to have lower vibrational energies than nonexchangeable ones,[31] in agreement with our present findings.

We now come to compare the spectra of the D_2O-hydrated and D_2O-hydrated deuterated samples. Once again, nonexchangeable protein hydrogens, contained in the D_2O-hydrated deuterated sample, show the anomalous excess of scattering, and the further contribution of exchangeable protein hydrogens, in the corresponding D_2O-hydrated sample, appears with a stronger scattering intensity. However, at variance with what was found for the dry samples, no peak frequency difference is apparent in this case.

For a more detailed analysis of the differences in the scattering intensity, we can refer, for instance, to the two desiccated samples. The spectrum of the dry sample $S_d(q,\omega)$ can be considered as a weighted average of the two dynamic structure factors of exchangeable and nonexchangeable hydrogen atoms:

$$S_d(q,\omega) = \frac{N_e}{N_e + N_{ne}} S_e(q,\omega) + \frac{N_{ne}}{N_e + N_{ne}} S_{ne}(q,\omega) \quad (6)$$

where the subscripts *e* and *ne* stand for exchangeable and nonexchangeable, respectively, whereas *N* indicates the number of hydrogen atoms of the relevant type. Notice that the three dynamic structure factors in eq 6 are all referred to a single hydrogen atom. $S_{ne}(q,\omega)$ is provided by the measured spectrum of the dry deuterated sample $S_{dd}(q,\omega)$. As the peak in $S_d(q,\omega)$ appears more intense than in $S_{dd}(q,\omega) = S_{ne}(q,\omega)$, the peak in $S_e(q,\omega)$ must be even stronger, resulting in a greater density of states at the energies of interest. Therefore, we can conclude that both surface and internal hydrogens give significant contributions to the scattering excess, but surface hydrogens are characterized by a higher number of accessible vibrational states, which could be related to a larger mobility of the outer

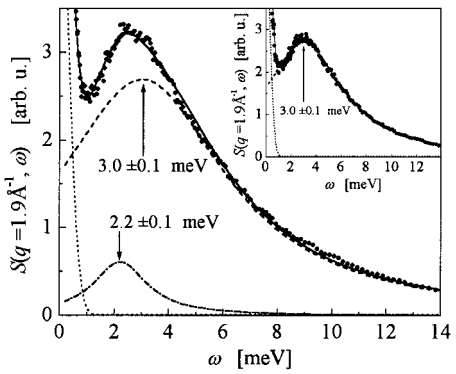

Figure 6. Dynamic structure factor, at $q = 1.9$ Å^{-1} and $T = 100$ K, of the dry sample (full circles). The full line is a fit of the experimental data. The fit function is the sum of three spectral components: an elastic line (dots), a lower-energy vibrational component due to exchangeable hydrogens (dots-dashes), and a higher-energy vibrational component due to nonexchangeable hydrogens (dashes). *Inset.* Dynamic structure factor, at $q = 1.9$ Å^{-1} and $T = 100$ K, of the dry deuterated sample (full circles). The full line is a fit of the experimental data. Besides the elastic line (dots), the spectrum consists of a single vibrational component due to nonexchangeable hydrogens (dashes).

protein shells with respect to the core. This latter indication is in agreement with a NMR relaxation study of βLG, which suggests that residues in the hydrophobic core are more rigid in contrast to the considerably higher flexibility of surface groups.[34]

We now draw attention to the frequency position of the anomalous peak. The spectrum of the dry deuterated sample, due to nonexchangeable protons only, was fitted with the sum of a Gaussian function, which reproduces the elastic resolution function of IN6, and a Lorentzian function, which reproduces the vibrational peak, describing a broad distribution of harmonic oscillators. As an outcome of the fitting procedure, the results of which are shown in the inset of Figure 6, a vibrational frequency $\omega_0 = 3.0 \pm 0.1$ meV was found for the inelastic scattering contribution from the nonexchangeable group of protons. Concerning now the dry sample, we can assume that its spectrum arises from the previous group of nonexchangeable hydrogens and by the additional group of exchangeable hydrogens. Therefore, to fit such spectrum, in addition to the 3 meV one, we took into account for the contribution of exchangeable hydrogens by another Lorentzian. Such an analysis revealed that the dry sample spectrum can be fully reproduced by two vibrational components, the first of which is peaked at the same frequency found for the deuterated sample (3.0 ± 0.1 meV), whereas the second is centered at the lower frequency of 2.2 ± 0.1 meV (see Figure 6).

The same kind of approach can be used for studying the differences between the two D_2O-hydrated samples. In this case, the two Lorentzians accounting for the contributions of exchangeable and nonexchangeable protons are found to be centered at frequencies which are equal within error bars: 3.2 ± 0.4 and 3.4 ± 0.1 meV, respectively (the results are summarized in Table 2). It should be remarked that the line width σ of the Lorentzian related to exchangeable hydrogens is so large that the contribution due to this atomic group appears as an almost flat extraintensity, rather than a separate and distinct vibration.

By resuming, in the dry samples, external residues appear to be characterized by lower vibrational frequencies with respect to internal ones, meanwhile in the hydrated samples, both kind of atomic groups display the same vibrational frequency.

The frequency shift, observed in the dry samples upon comparing the interior and the surface of the protein, can be phenomenologically discussed in the framework of the model ascribing the anomalous bump to phonon localization. Referring to eq 5, the same sound velocity v_s can be reasonably assumed for the dry and dry deuterated samples. Therefore, the higher vibrational frequency of internal residues can be attributed to a smaller correlation length D thus suggesting a phonon propagation confined within the inner protein shell. On the contrary, librations of surface groups would be characterized by larger correlation lengths, which result to be comparable with and slightly larger than the protein dimensions. Thus, the different vibrational frequencies of the two classes of protons seem to be consistent with the different volumes spanned by vibrations associated with such atomic groups. It can be therefore speculated about the fact that solvent-exposed side-chains, at the protein−protein interface, might mediate intermolecular interactions and thus be responsible for the propagation of vibrations across more than one molecule.

TABLE 2: Spectral Characteristics of the Two Hydrogen Classes, in Both Dry and D_2O-Hydrated Samples, Resulting from the Fitting Procedure (See Text)[a]

hydration state	H type	ω_0 (meV)	σ (meV)
dry	exchangeable	2.2 ± 0.1	1.2 ± 0.1
	nonexchangeable	3.0 ± 0.1	3.8 ± 0.1
D_2O-hydrated	exchangeable	3.2 ± 0.4	6.0 ± 0.4
	nonexchangeable	3.4 ± 0.1	3.9 ± 0.1

[a] ω_0 and σ represent respectively the center and line width of the Lorentzian function employed to model the vibrational peaks.

The observed different contributions to the anomalous peak might bear some relevance to the role of hydration water in the protein dynamics. Actually, we found that both surface and internal low-frequency motions are affected by the presence of the hydration shell, as, in the D_2O-hydrated samples, the vibrations of both exchangeable and nonexchangeable protons display the peak shift toward higher frequencies. Therefore, the plasticizing effect of water, which is known to trigger the large amplitude molecular motions, appears to act over the whole protein, rather than on its external surface only, in agreement with some recent experimental and simulative results.[47,48] Within the phonon localization model, this is further supported by the observation of the *same* vibrational frequency for both types of atomic groups. Indeed, same frequencies imply same correlation lengths D; thus, the vibrations of surface and buried residues seem to involve the same spatial domains. Therefore, at variance with what found in the dry protein, the connection between external groups and intermolecular vibrations and between internal groups and intramolecular vibrations cannot be easily established, therefore hydrated proteins appear to behave more likely as homogeneous media.

Conclusions

By means of inelastic neutron scattering, we have investigated the low-frequency dynamics of the globular protein β-lactoglobulin, on both dry and D_2O-hydrated samples. The measured low-temperature spectra are characterized by a scattering bump, peaking in the range 2−4 meV, which results to have a vibrational and incoherent nature. The derived densities of states witness that the bump is due to an anomalous excess of vibrational modes with respect to the harmonic Debye level.

Suitable H/D exchange procedures allowed us to discriminate between the dynamical behavior of exchangeable hydrogen atoms -mainly located in external residues- and nonexchangeable hydrogen atoms -situated in internal residues. In the desiccated

samples we could observe that a neat peak, centered at 3meV, is due to internal residues, in agreement with some simulative results.[46] Surface residues provide a further peak at lower frequencies and with a stronger intensity per scattering unit. In the hydrated samples, no frequency difference between the vibrations of surface and buried residues is found, whereas the difference in the scattering intensity is still observed.

The discussion of these results in the framework of a phonon localization model suggests the involvement of intermolecular vibrations. In particular, the higher vibrational frequency of internal residues is ascribed to the smaller volume, the hydrophobic protein core, spanned by their associated vibrations. On the other hand, surface residue vibrations, which are characterized by lower frequencies and consequently larger correlation lengths, are suggested to propagate across more than one molecule and to be thus connected with intermolecular interactions.

Hydration water is found to affect the low-frequency motions of both buried and solvent-exposed atomic groups. Therefore, the plasticizing effect of water, which is known to trigger large amplitude molecular motions, acts over the whole protein, rather than on its external surface only.[47,48] Moreover, in the framework of the phonon localization model, the finding of the same frequencies for both surface and internal residues implies that the respective vibrations propagate through the same spatial domains thus suggesting a picture of hydrated proteins as homogeneous media.

Acknowledgment. Institut Laue-Langevin in Grenoble is kindly acknowledged for having provided neutron facilities. The present work has been partly supported by a PRIN-MURST project.

References and Notes

(1) Smith, J. C. *Q. Rev. Biophys.* **1991**, *24*, 227.
(2) McCammon, J. A. *Rep. Prog. Phys.* **1984**, *47*, 1.
(3) Paciaroni, A.; Stroppolo, M. E.; Arcangeli, C.; Bizzarri, A. R.; Desideri, A.; Cannistraro S. *Eur. Biophys. J.* **1999**, *28*, 447.
(4) Cusack, S.; Doster, W.; *Biophys. J.* **1990**, *58*, 243.
(5) Diehl, M.; Doster, W.; Schober, H. *Biophys. J.* **1997**, *73*, 2726.
(6) Doster, W.; Cusack, S.; Petry, W. *Phys. Rev. Lett.* **1990**, *65*, 1080.
(7) Ferrand, M.; Dianoux, A. J.; Petry, W.; Zaccai, G. *Proc. Natl. Acad. Sci. U.S.A.* **1993**, *90*, 9668.
(8) Fitter, J. *Biophys. J.* **1999**, *76*, 1034.
(9) Brown, K.; Erfurth, S.; Small, E. W.; Peticolas, W. L. *Proc. Natl. Acad. Sci. U.S.A.* **1972**, *69*, 1467.
(10) Genzel, L.; Keilmann, F.; Martin, T. P.; Winterling, G.; Yacoby, Y.; Frölich, H.; Makinen, M. W. *Biopolymers* **1976**, *15*, 219.
(11) Buchenau, U. *Europhys. News* **1993**, *24*, 77.
(12) Angell, C. A. *Science* **1995**, *267*, 1924.
(13) Paciaroni, A.; Bizzarri, A. R.; Cannistraro, S. *Phys. Rev. E* **1999**, *60*, 1.
(14) Richter, D. *J. Phys.: Condens. Matter* **1996**, *8*, 9177.
(15) Engberg, D.; Wischnewski, A.; Buchenau, U.; Börjesson, L.; Sokolov A. P.; Torell, L. M. *Phys. Rev. B* **1998**, *58*, 9087.
(16) Frick, B.; Richter, D. *Science* **1995**, *267*, 1939.
(17) Wuttke, J.; Hernandez, J.; Li, G.; Coddens, G.; Cummins, H. Z.; Fujara, F.; Petry, W.; Sillescu, H. *Phys. Rev. Lett.* **1994**, *72*, 3052.
(18) Buchenau, U.; Wischnewski, A.; Richter, D. *Phys. Rev. Lett.* **1996**, *77*, 4035.
(19) Hehlen, B.; Courtens, E.; Vacher, R.; Yamanaka, A.; Kataoka, K.; Inoue, K. *Phys. Rev. Lett.* **2000**, *84*, 5355.
(20) Frauenfelder, H.; Parak, F.; Young, R. D. *Annu. Rev. Biophys. Chem.* **1988**, *17*, 451.
(21) Green, J. L.; Fan, J.; Angell, C. A. *J. Phys. Chem.* **1994**, *98*, 13780.
(22) Iben, I. E. T.; Braunstein, D.; Doster, W.; Frauenfelder, H.; Hong, M. K.; Johnson, J. B.; Luck, S.; Ormos, P.; Schulte, A.; Steinbach, P. J.; Xie, A. H.; Young, R. D. *Phys. Rev. Lett.* **1989**, *62*, 1916.
(23) Tirion, M. M. *Phys. Rev. Lett.* **1996**, *77*, 1905.
(24) Schirmacher, W.; Diezemann, G.; Ganter, C. *Phys. Rev. Lett.* **1998**, *81*, 136.
(25) Taraskin, S. N.; Loh, Y. L.; Natarajan, G.; Elliott, S. R. *Phys. Rev. Lett.* **2001**, *86*, 1255.
(26) Kantelhardt, J. W.; Russ, S.; Bunde, A. *Phys. Rev. B* **2001**, *63*, 064302.
(27) Elliott, S. R. *Europhys. Lett.* **1992**, *19*, 201.
(28) Das, S. P. *Phys. Rev. E* **1999**, *59*, 3870.
(29) Götze, W.; Mayr, M. R. *Phys. Rev. E* **2000**, *61*, 587.
(30) Paciaroni, A.; Bizzarri, A. R.; Cannistraro, S. *J. Mol. Liq.* **2000**, *84*, 3.
(31) Bizzarri, A. R.; Paciaroni, A.; Cannistraro, S. *Eur. Biophys. J.* in press.
(32) Papiz, M. Z.; Sawyer, L.; Eliopoulos, E. E.; North, A. C. T.; Findlay, J. B. C.; Sivaprasadarao, R.; Jones, T. A.; Newcomer, M. E.; Kraulis, P. J. *Nature* **1986**, *324*, 383.
(33) Monaco, H. L.; Zanotti, G.; Spadon, P.; Bolognesi, M.; Sawyer, L.; Eliopoulos, E. E. *J. Mol. Biol.* **1987**, *197*, 695.
(34) Kuwata, K.; Hoshino, M.; Forge, V.; Era, S.; Batt, C. A.; Goto, Y. *Protein Science* **1999**, *8*, 2541.
(35) Wu, S.-Y.; Perez, M. D.; Puyol, P.; Sawyer, L. *J. Biol. Chem.* **1999**, *274*, 170.
(36) Englander, S. W.; Kallenbach, N. R. *Q. Rev. Biophys.* **1984**, *16*, 521.
(37) Settles, M.; Doster, W. *Faraday Discuss.* **1996**, *103*, 269.
(38) Lovesey, S. *Theory of neutron scattering from condensed matter*; Oxford University Press: Oxford, 1986.
(39) Bée, M. *Quasielastic neutron scattering: principles and applications in solid-state chemistry, biology and material science*; Hilger: Bristol, 1988.
(40) Sokolov, A. P.; Novikov, V. N.; Strube, B. *Phys. Rev. B* **1997**, *56*, 5042.
(41) Cordone, L.; Ferrand, M.; Vitrano, E.; Zaccai, G. *Biophys. J.* **1999**, *76*, 1043.
(42) Bizzarri, A. R.; Paciaroni, A.; Cannistraro, S. *Phys. Rev. E* **2000**, *62*, 3991.
(43) Bellissent-Funel, M.-C.; Texeira, J.; Chen, S. H.; Dorner, B.; Middendorf, H. D.; Crespi, H. L. *Biopyhs. J.* **1989**, *56*, 713.
(44) Tarek, M.; Martyna, G. J.; Tobias, D. J. *J. Am. Chem. Soc.* **2000**, *122*, 10450.
(45) Steinbach, P. J.; Loncharich, R. J.; Brooks, B. R. *Chem. Phys.* **1991**, *158*, 383.
(46) Melchionna, S.; Desideri, A. *Phys. Rev. E* **1999**, *60*, 4664.
(47) Zanotti, J.-M.; Bellissent-Funel, M.-C.; Parello, J. *Biophys. J.* **1999**, *76*, 2390.
(48) Vitkup, D.; Ringe, D.; Petsko, G. A.; Karplus, M. *Nature Struct. Biol.* **2000**, *7*, 34.